Unveiling the Influence of Hydrated Deep Eutectic Solvents on the Dynamics of Water-Soluble Proteins

Journal:	*The Journal of Physical Chemistry*
Manuscript ID	jp-2023-00935h
Manuscript Type:	Article
Date Submitted by the Author:	10-Feb-2023
Complete List of Authors:	Parisse, Gianluca; Università degli Studi dell'Aquila Dipartimento di Scienze Fisiche e Chimiche Narzi, Daniele; University of L'Aquila, Belviso, Benny Danilo; Institute of Crystallography National Research Council Capriati, Vito; Universita degli Studi di Bari Aldo Moro, Farmacia-Chimica del Farmaco Caliandro, Rocco; Istituto de Cristallografia Consiglio Nazionale delle Ricerche, IC-CNR Trotta, Massimo; Consiglio Nazionale delle Ricerche, Istituto per i Processi Chimico Fisici Guidoni, Leonardo; Università degli Studi de L'Aquila, Departimento di Scienze Fisiche e Chimiche

Unveiling the Influence of Hydrated Deep Eutectic Solvents on the Dynamics of Water-Soluble Proteins

Gianluca Parisse[1], Daniele Narzi[1], Benny Danilo Belviso[2], Vito Capriati[3], Rocco Caliandro[*,2], Massimo Trotta[*,4], and Leonardo Guidoni[*,1]

[1]Department of Physical and Chemical Sciences, Università degli Studi dell'Aquila, I-67100 L'Aquila, Italy

[2]Istituto di Cristallografia, Consiglio Nazionale delle Ricerche, I-70126 Bari, Italy

[3]Dipartimento di Farmacia - Scienze del Farmaco, Università degli Studi di Bari "Aldo Moro", I-70125 Bari, Italy

[4]Istituto per i Processi Chimico Fisici, Consiglio Nazionale delle Ricerche, I-70125 Bari, Italy

[*]E-mail: rocco.caliandro@ic.cnr.it; massimo.trotta@cnr.it; leonardo.guidoni@univaq.it

Phone:+39 080 5929150

Abstract

Deep Eutectic Solvents (DESs) are solutions at liquid state made of hydrogen bond acceptors and donors mixed together in a specific molar ratio. These neoteric solvents are highly tunable through varying the structure or relative ratio of parent components and have been evaluated as solvents able to improve biomolecules's performance, specifically their stability and biocatalytic properties. Inspired by a recent crystallographyc study, we have explored through molecular dynamics (MD) simulations the dynamic properties of two different proteins (hen egg-white lysozyme and the human VH antibody fragment HEL4) in a (20% w/w) hydrated solution of Choline chloride – Glycerol (1:2). We have developed proper force fields to account for DES, protein and DES-Protein interactions, which have been calibrated using pair distribution function measurements of pure-DES solutions. MD results show that the presence of DES quenches the protein motion, increasing the rigidity of the overall protein structure. Specific interactions among DES components and protein residues, such as those between choline ions and two Tryptophan residues of lysozyme, may amplify the protein-DES interactions, and lead to

protein crystallization in the presence of hydrated DES. These findings open new horizons to enhance or achieve control on protein properties by a proper choice of hydrated DESs used as solvents.

1 Introduction

The most common solvents used in industry represent an important source of environmental pollution. The need of green alternatives to these solvents led to the search for more sustainable compounds. In this context, Deep Eutectic Solvents (DESs), first presented by Abbott and coworkers in 2003,[1] have gained considerable attention among the scientific community thanks to their eco-friendly character and easy preparation methods.[2] Besides, they show desirable properties such as low flammability, thermal and chemical stability and low vapour pressure that make them advantageous over organic solvents.[3]–[6] DESs are usually obtained by the right combination of a quaternary ammonium salt (Hydrogen Bond Acceptor - HBA) and a metal salt or Hydrogen Bond Donor (HBD). At the proper molar ratio the constituting species give rise to a eutectic mixture, for which the eutectic point temperature is lower than that of an ideal liquid mixture.[7] Depending on the nature of their constituents, DESs are classified into five main types (I-V). Most of them fall into types I-IV,[4] while non-ionic DESs belong to the recently proposed fifth type.[8]

Type III DESs, formed by Choline chloride and hydrogen bond donors, are certainly the most studied so far, mainly due to the ease of preparation, low cost and high biodegradability of the starting materials.[9]–[11] Among the HBD molecules studied to date, amides, carboxylic acids and alcohols have been often used to engineere deep eutectic solvents.[1], [12], [13] Due to the huge number of possible formulation, their physicochemical properties can be highly and easily tailored by choosing both the nature and the ratio of the constituents.[14] This has allowed DESs to be succesfully applied in several fields of science, such as electrochemistry,[15], [16] organometallics,[17]–[19] extraction and separation processes,[20]–[22] and biocatalysis.[10], [23]–[25]

Due to the high viscosity typical of DESs, limiting their practical application in many of these fields, it is common to use water as cosolvent in order to overcome this hindrance. This strategy is particularly useful in those cases where it would be inappropriate to work at high temperature. It is well known that the presence of water has an influence on the physicochemical properties and molecular arrangement of DESs. As reported in a recent review, many experimental and theoretical investigations were carried out to study the effect of water on physicochemical properties and nanostructure of DESs.[26] At low content, water seems to strengthen the DES's supramolecular network, while a higher content appear to weaken it. In-depth investigations by Edler and coworkers have shown that the nanostructure of the hydrated reline DES system is retained up to 42 wt% water.[27] Further addition of water brings DES-water systems to become aqueous solutions of HBA and HBD. [28]–[30]

The current interest in DESs in biocatalysis arises from having found them to be nondetrimental when used as solvents for biomolecules.[31]–[33] This means that, in principle, these solvents in both their pure and hydrated forms can be used as alternatives to the traditional organic solvents in order to carry out biotransformation processes. In addition, hydrated DESs were found to allow protein crystallization, also confering a major stabilization to the risulting crystal.[34] This is very attractive, since the use of stable crystals containing biomolecules as immobilization strategy could be implemented for biotechnological applications.[35] Sanchez-Fernandez and coworkers have recently shown that lysozyme remains stable up to 40 days of storage in pure 1:2 choline cloride:glycerol at room temperature.[36] Despite the increased interest and their benign and economically viable nature, only a limited number of studies on the effect of pure and hydrated DESs on protein structures have been carried out so far. To date, most of the studies performed on DES-protein systems involve lysozyme, a common globular antimicrobial enzyme. Experimental investigations showed that the presence of water plays a key role in preserving the protein folding, maintaining the enzymatic activity.[37], [38] Beyond these observations, there is

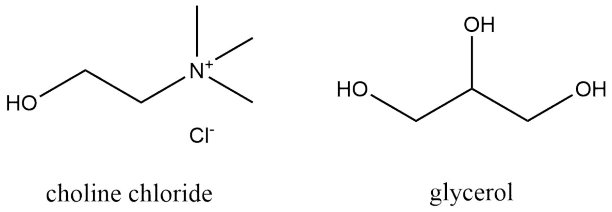

choline chloride glycerol

Figure 1: Chemical structure of the constituting species of the studied deep eutectic solvent

much more to know about the specific interactions between proteins and DESs. As recently reported by Kumari et al.[39], MD simulations are a powerful tool to get insights about the impact of pure and hydrated deep eutectic solvents on protein structure and conformation, also predicting their dynamic properties. However, due to their strong interactions, DESs are very challanging to describe from a theoretical point of view, especially as for their dynamic properties.[40]

Nowadays, the most common practice implemented to theoretically reproduce properties of DESs in a classical mechanics framework, is to apply a scaling factor to the atomic charges defined in the respective force field (FF). This requires to compute first partial charges for each species. Atomic charges can be obtained either from the most stable conformation in the gas phase of each isolated species or from the minimal cluster of eutectic composition for each system.[41]–[45] Recently, Chaumont and coworkers have shown an alternative method of FF development for pure DES solvents, based on Lennard-Jones (LJ) refinement.[46] This second approach could allow to make DES force fields compatible with the most common force fields used in the last decades for biomolecules. In the present study, we used a novel approach to model DES-water-protein interactions by treating separately the LJ parameters for DES-water/DES-protein interactions and for DES-DES interactions. Using such scheme, the effect of the pure Choline chloride – Glycerol DES (see Figure 1) or aqueous solutions of Choline chloride – Glycerol DES on the structural dynamics of two proteins was investigated by using MD simulations. First we validated the three force fields used through MD simulations carried out on pure DES and its hydrated mixture. Then, we explored the impact of a Choline chloride – Glycerol/water mixture at high DES content (80% w/w) on the conformation and stability of hen hegg white lysozyme (HEWL) and human VH antibody domain (HEL4). Proteins, DES and its hydration level have been choosen referring to the recent work published by Belviso et al.[34] with the aim of predicting the reasons that trigger protein crystallization in the presence of deep eutectic solvents. The three force fields used to model DES-water-protein interactions display qualitatively equivalent results, making the reported data more robust.

2 Methods

All MD simulations were carried out using the GROMACS software package.[47], [48] All the simulation boxes containing the deep eutectic mixture $[Ch]^+[Cl]^-$ – glycerol (1:2) were generated using the PACKMOL package.[49] Figure 1 shows the molecular structure of the DES components: Choline Chloride and glycerol.

2.1 Simulated systems

DES Choline chloride – Glycerol (1:2) To prepare the pure system, the deep eutectic solvent's constituting species were randomly placed into a cubic simulation box of side $\sim$ 60 Å. The choline cation $[Ch]^+$ and the chloride anion Cl^- were inserted independently from each other, according to the molar ratio of the DES.

DES-water mixtures As for pure DES, in DES-water mixtures the DES species were randomly placed into twelve simulation cubic boxes (box length $\sim$60 Å) of different water content (% w/w).

Proteins The initial structures of hen egg white lysozyme (PDB 1AKI)[50] and human VH antibody domain (PDB 7OBF) were taken from the RCSB Protein Data Bank. The two proteins were solvated either in water or in DES-water mixture (80/20 % w/w) into cubic boxes of side 85.4 Å and 95.7 Å, respectively. In water, Na^+ and Cl^- were added to

the systems at physiological concentration (0.15 M). An excess of Cl^- ions were used to neutralize the net positive charge of lysozyme, exept for the $FF_{\pm 0.92e}$ simulation in which F^- were used instead due to the scaling factor applied to the DES's ionic species $[Ch]^+$ and Cl^-. In the case of human VH antibody domain, Na^+ ions were used to neutralize the net negative charge of the simulated systems.

2.2 Force Field parameters

In the present work two different force fields were used to describe the pure DES: one developed by solely refining Lennard-Jones parameters of the hydroxyl function atoms and the other following the most common practise for DES of charge scaling. FF parameters of the former (FF_{LJ}) were taken by a recent work published by Chaumont et al.[46] whereas for the latter strategy we developed our own force field ($FF_{\pm 0.92e}$). FF parameters for the choline cation ($[Ch]^+$) and for the glycerol molecule were taken from the General Amber Force Field (GAFF) v2.11,[51] designed for simulation of small molecules. The force field parameters for the chloride anion (Cl^-) were obtained from AMBER03.[52] Atomic charges for $[Ch]^+$ and glycerol atoms were obtained using the standard RESP procedure on the optimized geometry in the gas phase of each isolated species using the Gaussian16 software package.[53] Geometry optimizations were carried out using the B3LYP/6-31G* method and then calculating the electrostatic potential on the optimized structures using the HF/6-31G* method. To obtain a better agreement with experimental results,[54], [55] we used an empirical approach testing some different scaling factor to use on the partial charges of the ionic species. The best agreement has been achieved when using a reduced charge of $\pm 0.92e$ for the ionic species.

For the description of DES-water and DES-water-protein systems, a third force field (FF_{mix}) was taken into account, developed following a novel approach based on the idea of treating separately DES-DES and DES-water-protein interactions. In order to implement such a strategy, we acted on Lorentz-Berthelot combination rules used to construct cross terms in vdW interactions (eqs (1) and (2)).

$$\sigma_{ij} = \frac{\sigma_i + \sigma_j}{2} \tag{1}$$

$$\epsilon_{ij} = \sqrt{\epsilon_i \epsilon_j} \tag{2}$$

Since this implies to act on Lennard-Jones parameters, we used those from Chaumont's work to describe DES-DES interactions,[46] while DES-water and DES-protein interactions were modeled using the original non-bonded parameters of the GAFF v2.11 [51] for *oh* and *ho* atom types (i.e. oxygen and hydrogen atoms of the hydroxyl groups). Chaumont and coworkers took FF parameters for the $[Cl]^-$ from the work of Cheatham et al.[56] which were optimised for SPC/E water model. In this work, we used TIP3p water model,[57] so it was more appropriate to use the original non-bonded parameters of AMBER03 [52] for the chloride $[Cl]^-$ anion when interacting with proteins and water molecules.

2.3 Molecular Dynamics simulations

After minimization with the steepest descent algorithm, we equilibrated the system for 100 ns in the NVT-ensemble. Then, 200 ns MD simulations were performed in NpT ensemble. Long range electrostatic interactions were computed by the Particle Mesh Ewald (PME) method,[58] using a grid spacing of 0.12 nm and a short range cutoff of 1.2 nm. The LINCS algorithm [59] was used to constrain all the hydrogen-involving bonds. A step size of 2 fs was used for numerical integration of the equations of motion. The temperature was kept constant at 298.15 K using the V-rescale algorithm [60] and the systems were isotropically coupled to a pressure bath at 1 bar, using Parrinello-Rahman barostat.[61], [62]

In case of protein simulations, all equilibrium MD simulations were preceded by energy minimization using the steepest descent algorithm, followed by 20 ns of MD simulations with harmonic position restraints (force constant 1000 kJ mol^{-1} nm^{-2}) applied on protein's heavy atoms in NVT ensemble in order to equilibrate the solvent. Finally, 200 ns of unrestrained MD simulations were carried out in NpT ensemble at 1 bar, using Parrinello-Rahman barostat.[61], [62] The Nosé-Hoover algorithm was used

to keep the temperature constant at 298.15 K.[63], [64]

2.4 Pair distribution function (PDF)

PDF measurements were performed at the National Synchrotron Light Source (NSLS-II) of the Brookhaven National Laboratory. The 28ID-2 beamline was used, with a primary X-ray beam of 74.52 keV (0.1664 Å) energy and 0.5 mm x 0.5 mm spot size. A Perkin Elmer XRD 1621 digital imaging detector (2048 x 2048 pixels of 200 x 200 µm size) orthogonal to the beam was put 202 mm downstream the sample to optimize PDF measurements. Nickel was measured as a standard reference material to calibrate the wavelength and the detector position/orientation. The DES sample was put in a Kapton tube of 2 mm diameter. An empty capillary similar to that used for holding the DES sample was measured for background estimation. X-ray measurements were performed at room temperature, with no filters and by spinning the sample. Diffraction images were azimuthally integrated and converted into intensity profiles versus 2 θ and versus momentum transfer (Q) by using the FIT2D program.[65] PDF profiles were calculated up to interatomic distances r of 20 Å from Q profiles by the program PDFGetX3.[66] The parameters for PDF calculation (background subtraction scale factor, minimum and maximum values of Q, degree of data-correction polynomial) were optimized to reduce termination effects and to enhance the signal to noise ratio. The Qmax parameter was set to 17.0 $Å^{-1}$. The PDF profile was refined by using a python script based on the DiffPy-CMI library.[67] The last frame from the simulation of pure Choline chloride – Glycerol DES with the FF_{LJ} force field and the $FF_{\pm 0.92e}$ force field was used as fitting model. All the atoms included in the 6x6x6 nm box were considered, apart from the hydrogen atoms, to speed up calculations. The fits were executed in the range of interatomic distances from 0.5 Å to 13 Å, which includes all the features of the PDF profile, with a step of 0.01 Å. The fitting model was defined as the convolution of the PDF contribution due to a bulk crystal structure and that due to the crystal shape. The model parameters were refined separately, i.e. by keeping constant all the others, with the following order: scale factor, peak shape parameters: Qbroad, (peak broadening from increased intensity noise at high Q) and delta1 (coefficient for 1/r contribution to the peak sharpening), isotropic displacement factors. Three atomic displacement parameters were considered and refined separately: one for the Cl^- ions, one for the non-hydrogen atoms of the choline ion, and one for non-hydrogen atoms of the glycerol molecule. The crystal shape was assumed spherical with a diameter of 10 nm (parameter not refined) and the atomic positions were kept fixed. 10 refinement cycles implementing this protocol were performed.

2.5 MD calculated properties

Density (ρ) values were obtained by averaging the results over the last 25 ns of MD in the NpT ensemble.

Self-Diffusion Coefficients for the choline ions ($[Ch]^+$), the Cl^- ions and glycerol molecules (GOL) were calculated over the NpT trajectories using the Einstein relation (eq(3)).[68]

$$\lim_{t\to\infty} \langle ||\mathbf{r_i(t)} - \mathbf{r_i(0)}||^{\mathbf{2}} \rangle_{\mathbf{i\in A}} = \mathbf{6D_A t} \qquad (3)$$

D_A is the self-diffusion coefficient of type A particles, $\mathbf{r_i}$ is the position of the i-th A type particle at time t.

Radial distribution function (RDF) or pair correlation function $g_{AB}(r)$ between particles of type A and B is defined as follows:

$$g_{AB}(r) = \frac{\langle \rho_B(r) \rangle}{\langle \rho_B \rangle_{local}} = \frac{1}{\langle \rho_B \rangle_{local}} \frac{1}{N_A} \sum_{i\in A}^{N_A} \sum_{j\in B}^{N_B} \frac{\delta(r_{ij} - r)}{4\pi r^2}, \qquad (4)$$

where $\langle \rho_B(\mathrm{r}) \rangle$ is the density of particles B at a distance r around particles A, $\langle \rho_B \rangle_{local}$ is the density of type B averaged over all spheres around particles A with radius r_{max}. RDFs between the center of mass (COM) of the DES species $[Ch]^+$,Cl^- and GOL were calculated over the MD trajectories in the NpT ensemble.

2.6 Dynamical Cross-Correlation Matrix (DCCM)

We assessed the correlated motion between residues by means of the the Dynamical Cross-Correlation Matrix (DCCM), which measures the cross-correlations of atomic displacements. Calculations have been performed by using VMD,[69] with a tcl script that performs: (i) a frame-by-frame alignment of the structural models within the trajectory considering only C_α atoms: (ii) a calculation of the Pearson's linear coefficient of the vectorial displacements of C_α atoms with respect to their average positions, according to the equation:

$$corr\left(\vec{r},\vec{s}\right)=\frac{\sum_{k=1}^{N}\left(\vec{r_k}-\langle\vec{r}\rangle\right)*\left(\vec{s_k}-\langle\vec{s}\rangle\right)}{\sqrt{\sum_{k=1}^{N}\left(\vec{r_k}-\langle\vec{r}\rangle\right)^2\sum_{k=1}^{N}\left(\vec{s_k}-\langle\vec{s}\rangle\right)^2}} \quad (5)$$

where $\vec{r}$ and $\vec{s}$ are the vector positions of two C_α atoms of the protein, k=1,...N identifies the frame of the MD trajectory and the $*$ operator indicates the scalar product between the two displacement vectors. The DCCM maps have been plotted by using the ROOT package.[70]

3 Results and Discussion

Before proceeding with the simulations of proteins in 80/20 (% w/w) DES/water mixture, the force fields used to describe Choline chloride – Glycerol (1:2) DES and its aqueous mixtures were validated against available experimental and theoretical values. In this regard, we computed densities, self-diffusion coefficients and radial distribution functions comparing our results with both experimental[54], [55], [71]–[73] and computational studies.[43], [46]

The results obtained in this study appear in good agreement with that found in the literature, thus confering reliability to the force fields used. Looking at the computed densities as function of the hydration level of the DES mixture (Figure S2, Table S5) it is noteworthy underlining a better agreement of the FF_{mix} with the experimental values compared to the other FFs used. Additional details are shown in the Supporting Information (Figures S1 and S2; Tables S1-S5).

Pair Distribution Function (PDF) results Since the FF_{LJ} model was identified as the basis for the development of FF_{mix}, further experimental validation was performed through X-ray diffraction measurements performed in PDF mode. The pure DES models have been validated against experimental PDF data, which monitor the local order in amorphous or quasi-crystalline materials. As shown in Figure 2, the PDF profile calculated from the last frame of the FF_{LJ} simulation (Figure 2a) has a better agreement with data than that calculated from the $FF_{\pm 0.92e}$ simulation (Figure 2b). In particular, FF_{LJ} is able to reproduce the small-range features of the PDF profile, i.e. all its sharp peaks comprised between 1 and 4 Å better than $FF_{\pm 0.92e}$. The discrepancies at interatomic distances smaller than 1 Å are due to finite-size artifacts and are not significant. The fitting parameters are summarized in Table 1. The agreement factor with data (R_w) is slightly better for FF_{LJ} than $FF_{\pm 0.92e}$ models.

For both fits, the peak shape parameters assume realistic values for PDF refinements, and the atomic displacement parameters are consistent with expectations, showing much higher mobility of the Cl^- with respect to choline ions and glycerol molecules, and chlorine ions fluctuating more than glycerol. On the basis of the results reported, FF_{LJ} is more suitable to simulate the Choline chloride – Glycerol (1:2) DES, and pure DES simulations can be considered fully validated by X-ray diffraction experimental data sensitive to the chemical short-range order.

3.1 Lysozyme

Recently Belviso and coworkers succesfully achieved crystallization of lysozyme using three different choline eutectic mixtures, including Choline chloride – Glycerol (1:2) at low hydration level.[34] In this context, four MD simulations of lysozyme, one in water and three in 80/20 (% w/w) DES/water mixture using three different force fields, were carried out starting from the crystal structure.

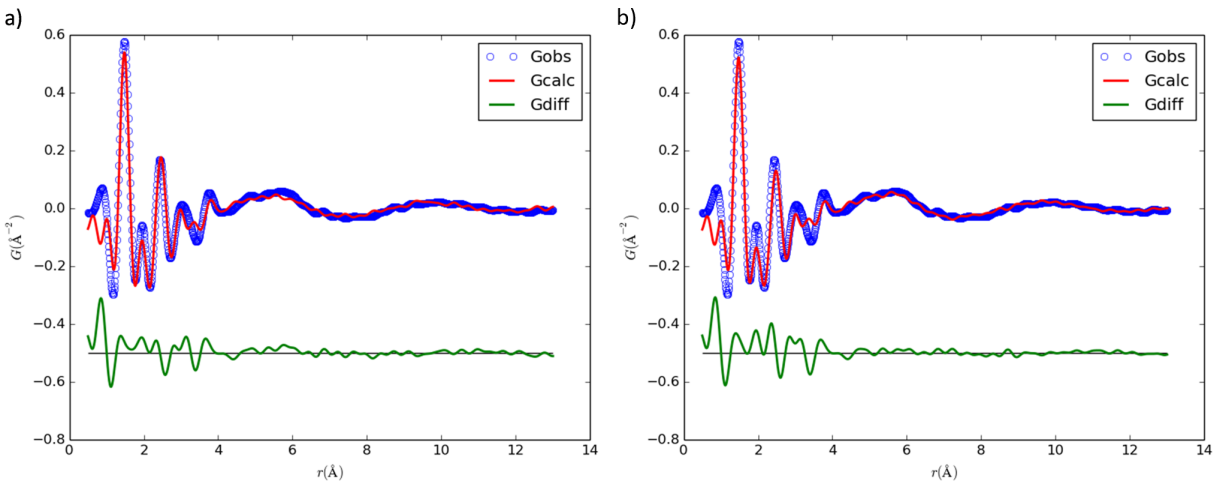

Figure 2: Results of the fit of pair distribution function experimental data with the final frame of the pure DES model simulated by the FF_{LJ} (a) and $FF_{\pm 0.92e}$ (b) force fields. Experimental (blue dots), calculated (red line) and difference (green line) PDF values are shown.

Table 1: Refinement parameters of the PDF fit. R_w is the weighted agreement factor between observed and calculated PDF, Delta1 is the coefficient for 1/r contribution to the peak sharpening, Q_{broad} describes the peak broadening from increased intensity noise at high Q, B are the thermal factors of the Cl^- ion and the of the atoms of the choline ion $[Ch]^+$ and the glycerol molecule (GOL).

Parameter	$\mathbf{FF}_{LJ}$	$\mathbf{FF}_{\pm 0.92e}$
R_w	0.331	0.363
$Delta1$	1.23	1.38
Q_{broad}	0.07	0.133
$B(Cl^-, [Ch]^+, GOL)(Å^2)$	$42.684, 0.001, 0.082$	$6.67, 0.489, 0.003$

3.1.1 Overall stability

We evaluated the overall stability of lysozyme in water and DES-water mixture by computing different properties as function of time (see Figure 3). Top panel shows the RMSD of atoms of the whole HEWL backbone with respect to its reference structure either in water and in 80/20 (% w/w) DES-water mixture. RMSD values in water lay in the range of 0.1-0.25 nm. Differently in DES aqueous mixture these values slightly decrease and, more importantly, remain constants below 0.1 nm all over the simulation time. This suggests that the hydrated DES solvent tends to preserve the original protein structure.

The radius of gyration allows us to understand the effect of the DES on the compactness of protein structure. As reported in Figure 3 both water and DES-water mixture do not affect the compactness of lysozyme. The Rg values lie around the average value of 1.4 nm in both solvents.

Finally, calculating the total number of hydrogen bonds present in the whole protein as a function of time, it appears clear that the presence of DES does not affect the stability of the secondary structures.

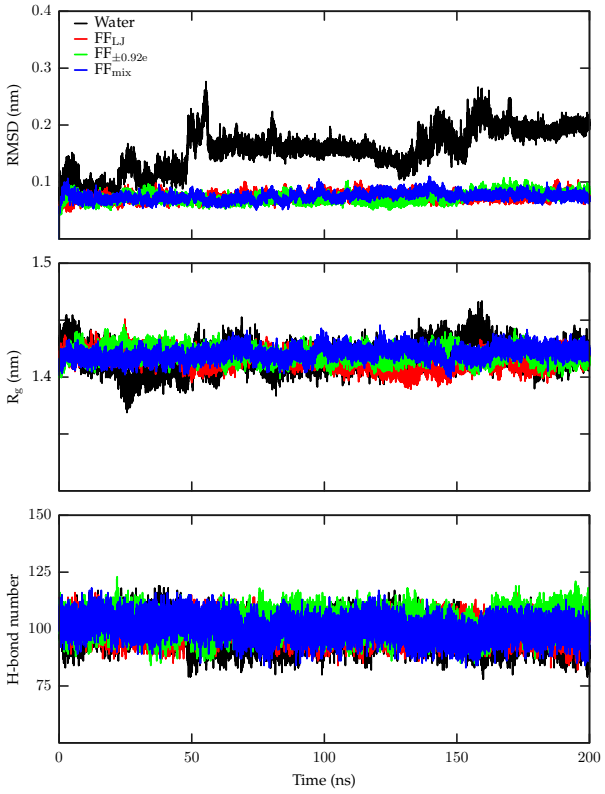

Figure 3: Impact of 80/20 (% w/w) DES/water mixture on lysozyme compared to water From top to bottom panel: RMSD calculated on the protein backbone with respect to its crystal structure as function of time; variation of radius of gyration (R_g) of lysozyme during simulation; total number of lysozyme's hydrogen bonds computed over the whole trajectory.

In addition, the simulations in water and in 80/20 (% w/w) DES/water mixture display similar results, thus confirming that DES does not affect the secondary structures.

The three analyses discussed above show an interesting behaviour: lysozyme in hydrated DES shows a rigidity higher than the rigidity of the protein in pure water. We decided to further investigate this aspect by computing the RMSF of C_α atoms for each residue of HEWL in water and 80/20 (% w/w) DES/water mixture. In water solution, the observed RMSF values are lower than 0.1 nm for most of the residues (Figure 4). A higher RMSF value is found in correspondence of the loops including residues 14-22, 46-50 and 121-124, indicating that in water these regions are more flexible than the rest of the protein. In hydrated DES, the rigidity of lysozyme is, in average, comparable to the rigidity in water with the exception of the above mentioned residues.

The presence of DES affects the correlated motion within the protein, as determined by the Dynamical Cross-Correlation Matrix (DCCM) (Figure 5). Coupled fluctuations of atomic positions usually occur among neighboring residues, so that DCCM matrices are always peaked along its main diagonal. However, longer-ranges correlations are also present, which in lysozyme mainly affect two regions, shown in Figure 5b: the β-hairpin comprising residues 37 to 58 (in blue) and the loop region comprising residues 59-78 (in red). The combined motion of these two regions is crucial for the protein to carry out its function, as they represent the lid that opens on the lower domain to perform the bacterial lysis. Diffuse off-diagonal correlations are also present for the longer α-helix (in green), whose movements are propagated to neighboring regions.

A general decrease in the variability of correlation values determined by eq.(5) is observed in hydrated DES (Figure 5c) with respect to the pure water (Figure 5a). In these conditions, the protein motion is smoothed by DES viscosity, so that correlated fluctuations among backbone atoms are reduced. As a result, extreme positive and negative correlation values are absent in the DCCM of Figure 5c, and the correlated motion of the longer α-helix is highly reduced.

On the other hand, the characteristic off-diagonal peaks due to the functional movements between the blue and red regions described above are still evident, suggesting that in hydrated DES the activity of the protein is not jeopardized notwithstanding the overall increase of its rigidity.

A numerical assessment of these observations, reported in the Supporting Information (Figure S3), shows that the presence of DES reduces by about 30% the average absolute value of the dynamic cross-correlation and this reduction affects equally the di-

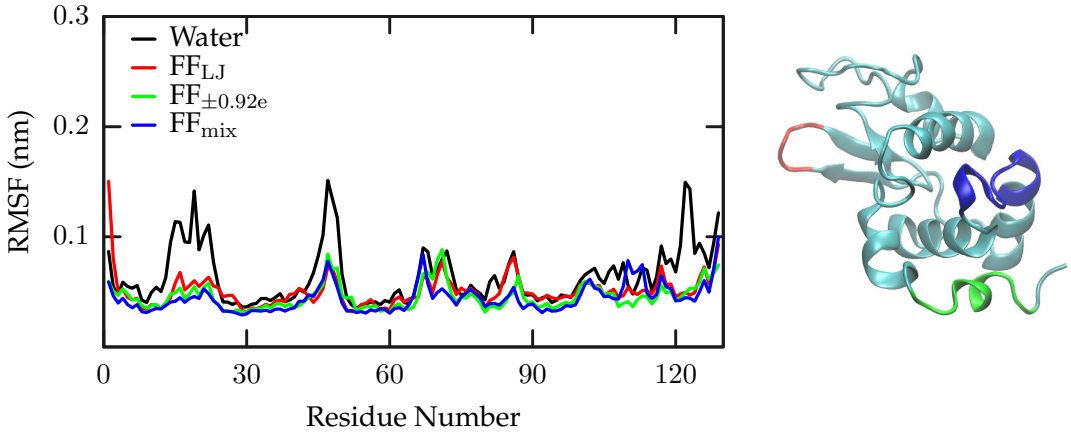

Figure 4: RMSF values of C_α of each HEWL's residue over the last 25 ns in water and 80/20 (% w/w) DES/water with the three FFs used in this study. The most flexible residues in water are coloured on the protein model.

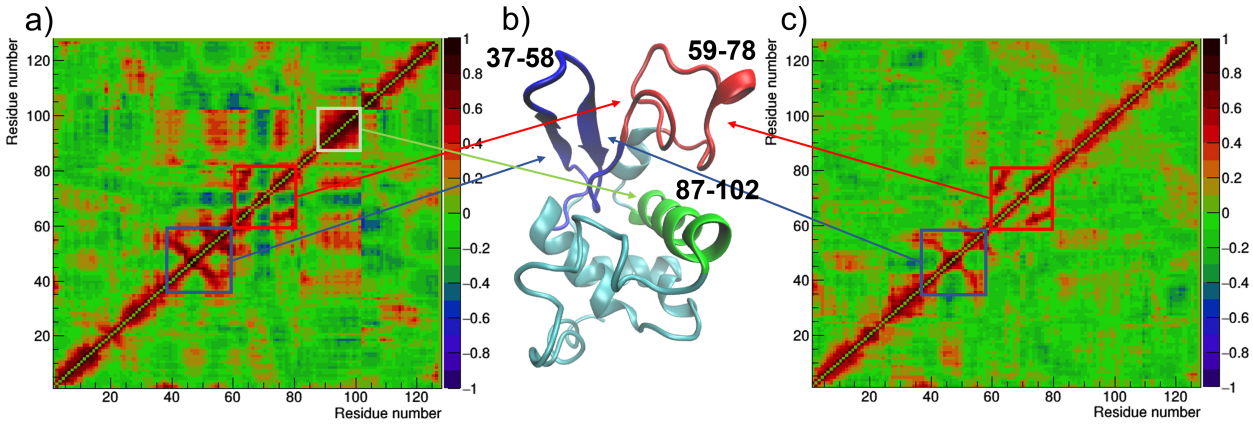

Figure 5: DCCMs calculated for simulations of HEWL in water (a) and DES parametrized by FF$_{mix}$ (c). Three regions of the protein showing higher off-diagonal correlations are highlighted by squares in a) and c), and coloured on the protein model in b), by using the same colour of the squares.

agonal and the off-diagonal region of the DCCM matrix. It is worth noting that similar results have been obtained by all the force fields used to describe DES interactions (Figures S3 and S4).

3.1.2 DES-protein interactions

Given the presence of the choline cation in the crystal structure, Belviso et al. work suggests the existence of two binding sites for $[Ch]^+$.[34] Both are dominated by π-cation interactions between choline and Trp62 and Trp123 residues, respectively. The authors attribute a key role for these DES-protein interactions during the crystallization process. Following their hint, we tested if these $[Ch]^+$-Trp interactions occur also in the simulated trajectories. An example of interactions between choline cations and Trp62 and Trp123 residues occuring along our simulated trajectories are shown in Figure 6.

In this regard, the minimum distances sampled

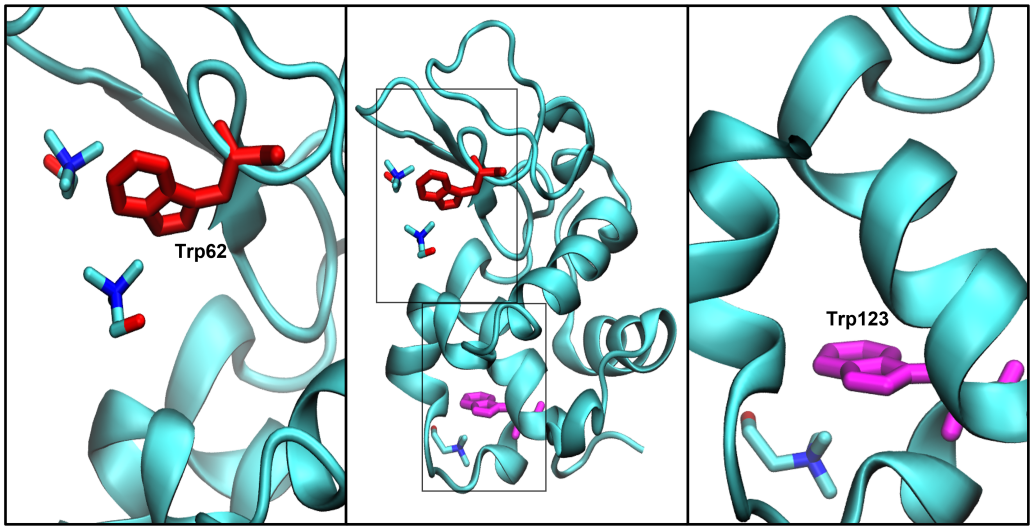

Figure 6: Choline sites in lysozyme Both choline sites show the presence of at least one $[Ch]^+$ at a minimum distance of 2 Å. Choline ions in the two sites interact with Trp.

along the MD simulations between Trp123 and $[Ch]^+$ have been calculated and are reported in Figure 7. The two tryptophans interact very similarly with the choline cation and the results for the interaction Trp62-$[Ch]^+$ are shown in the Supporting Information (Figure S5). Figure 7 shows that there is always at least one choline cation at 2 Å from Trp123 during the whole simulation time, strongly suggesting the existence of specific $[Ch]^+$-protein interactions. The same trend as shown in Figure 7 was observed for each of the different force fields used. Our results suggest that the aqueous mixture of DES has an impact on lysozyme behaviour by means of specific interactions DES-protein.

The enhanced rigidity related to the high viscosity of the hydrated DES solvent, combined with the specific interaction between triptophan and choline ions, can be considered as molecular determinants responsible for lysozyme crystallization in the presence of hydrated DES. We hence performed the calculations under the same conditions of temperature and pressure on a different protein, the human VH antibody domain, to highlight if the enhanced structural rigidity is peculiar of lysozyme or it is more general.

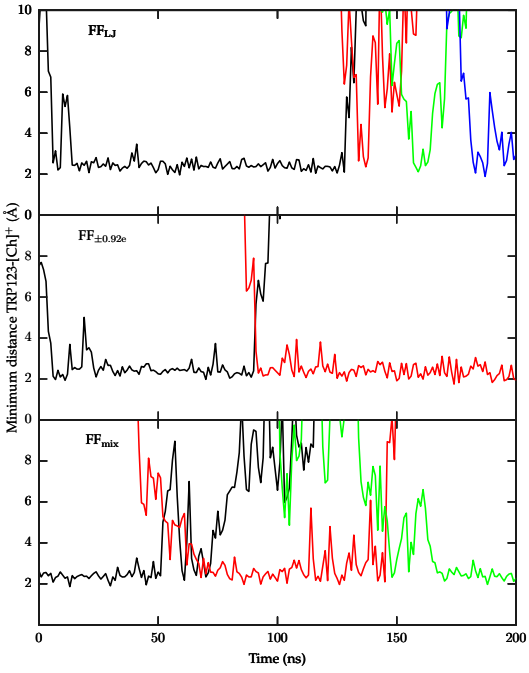

Figure 7: Minimum distance Trp123-$[Ch]^+$ over the whole trajectory. From top to bottom panel: FF_{LJ}; $FF_{\pm 0.92e}$; FFmix

3.2 Human VH antibody domain

Human VH antibody domain is a dimer with a prevailing β-sheet secondary structure tested by Belviso and coworkers,[34] whose crystal structure in hydrated DES could not be obtained.

3.2.1 Overall stability

As for lysozyme, we evaluated the overall stability of human VH antibody domain (HEL4) by calculating as a function of time, RMSD, radius of gyration and H-bond number. Figure 8 reports the RMSD values for the entire protein and both the two chains constituting the dimer.

It is noteworthy underlining that hydrated DES is not detrimental to the HEL4 tertiary structure and yet, the presence of the DES components makes the protein more rigid. However, hydrated DES solvent shows a lower impact compared to that found for lysozyme.

The analysis of radius of gyration shows, in both water and 80/20 (% w/w) DES/water mixture, an overall stability of the size of HEL4. It can be seen from Figure S6 that R_g values of the protein remain constant around an average of 1.8 nm in water and in hydrated DES mixture. This suggests that HEL4 is able to maintain its compactness throughout the simulations even in the presence of DES.

The number of intra and inter-monomer H-bond interactions slightly tend to increase, suggesting that secondary structures are preserved over the simulation time. Apparently the presence of DES leads to the same results obtained in water (Figure S7).

Finally, we focused our attention on the protein flexibility. It is worth noting that the presence of DES contributes to suppress the mobility of some residues (see Figure 9). In water, the majority of protein residues present RMSF values lower than 0.1 nm, suggesting that HEL4 is mostly rigid. The only two peaks worth mentioning are related to residues 25-32 of chain A and residues 100-106 of chain B. The presence of DES "freezes" the whole protein as can be seen from the fact that all RMSF values are lower than 0.1 nm.

The study of correlated fluctuations of HEL4

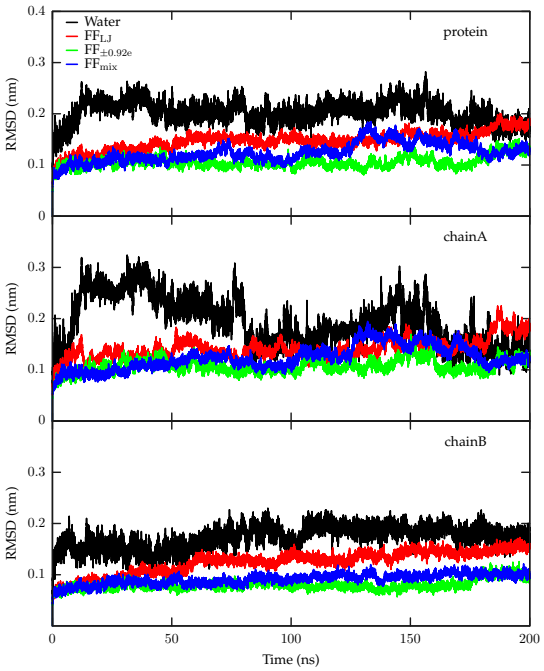

Figure 8: RMSD calculated on the backbone with respect to the starting structure. From top to bottom panel: protein; chainA; chainB

shown in Figure 10 clearly indicates that the regions corresponding to the two chains exhibit strong intra-dimer cross-correlations in the DCCM. For the simulation in water (Figure 10a), relevant inter-dimer cross-correlations are also present, and the two chains of the dimer have an asymmetric behavior, with the shorter chain B showing higher correlated motion than the longer chain A (Figure 10b). Both the amount of correlated motion and the asymmetric behavior within the dimer are reduced in the presence of DES, whereas the inter-dimer cross-correlations are almost absent (Figure 10c). This confirms the damping effect of correlated motion introduced by the DES solvent, which can be estimated as 40%, independently of the force field used (Figures S8 and S9).

The effect of reduction of the asymmetry between the two chains of the dimer in the hydrated DES solvent with respect to the pure water solvent is instead

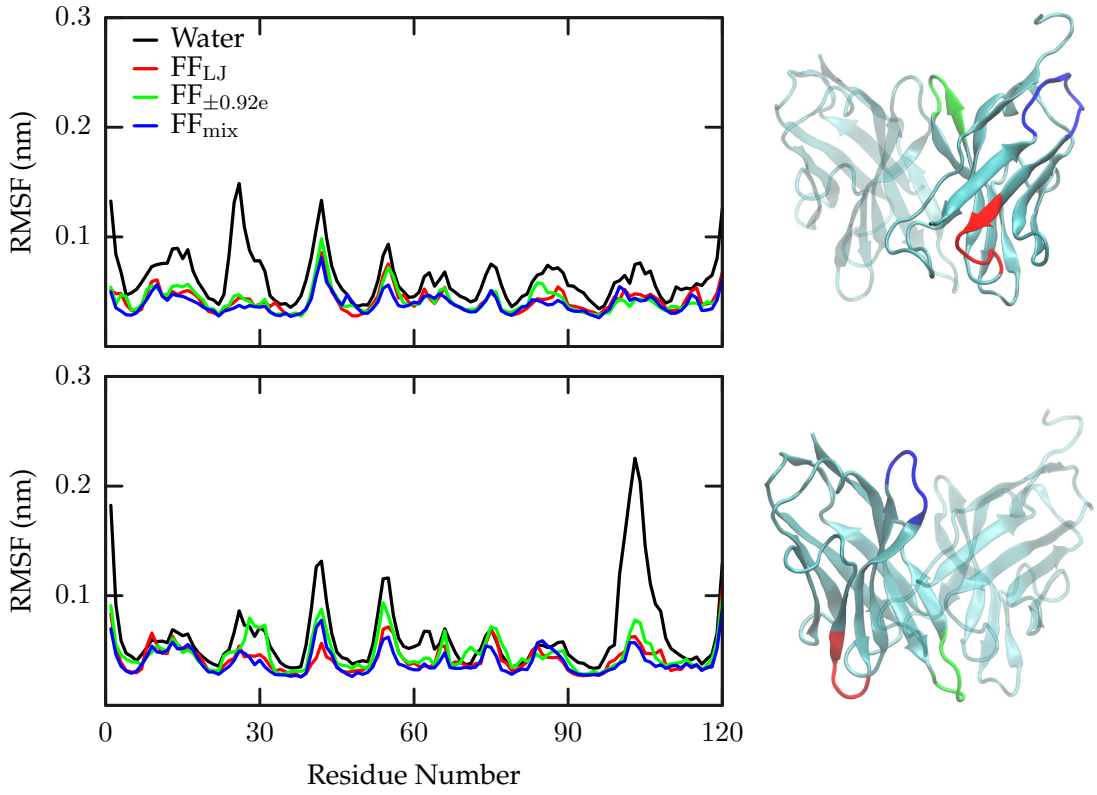

Figure 9: RMSF of C_α of each HEL4's residue over the last 25ns in water and in 80/20 (% w/w) DES/water with the three FFs used. The most flexible residues in water are coloured. Top panel chainA; bottom panel chainB.

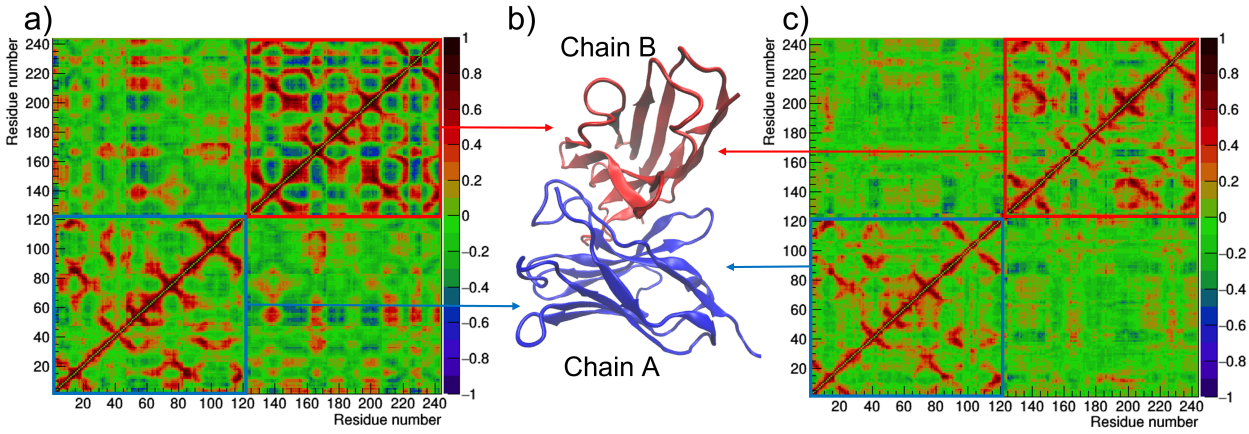

Figure 10: DCCMs calculated for simulations of HEL4 in water (a) and DES parametrized by FF$_{mix}$ (c). The two chains of the HEL4 dimer are highlighted by squares in a) and c), and coloured on the protein model in b), by using the same colour of the squares.

estimated as 20%, independently of the force field used (as shown in Figure 11).

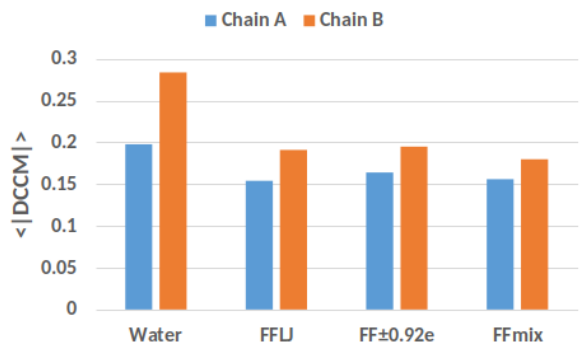

Figure 11: Averages of the absolute dynamical cross-correlation value calculated separately for chain A and chain B of the HEL4 dimer, calculated in water and in DES parametrized by the FF_{LJ}, $FF_{\pm 0.92e}$ and FF_{mix} force fields.

Conclusions

In this article, we present a throughout investigation of the influence of the hydrated deep eutectic solvent Choline chloride – Glycerol (1:2) on the structure of two water soluble proteins, namely lysozyme and Human VH antibody domain. To the purpose, molecular dynamics simulations were run, developing - when needed - appropriate force fields suitable for the accurate description of the interacting systems. The simulated DES properties fairly agree with Pair distribution function and Dynamical Cross-Correlation Matrix obtained from X ray synchrotron experiments. The comparison between protein/water and protein/DES/water MD simulations and experimental data shows that the presence of hydrated DES does not jeopardize the secondary and tertiary structures of the two proteins even if the flexibility of specific groups of amino acids is firmly reduced. Moreover, the dynamics of the choline cations reported in the crystallographic structure of the Choline chloride – Glycerol (1:2) hydrated DES was investigated. The results here reported show that the interaction between two specific tryptophans and the choline cation may be playing a central role in the improved crystallization of lysozyme in hydrated DES, confirming the hypothesis previously formulated.[34] We believe that the present work represents a step forward in the understanding of the unusual properties shown by hydrated DES in improving protein stability and allowing the protein crystal formation. Further investigations are needed to reveal similarities between the behaviour of lysozyme and other hydrated DESs or between other water soluble or membrane proteins and the hydrated Choline chloride – Glycerol (1:2).

Supporting Information

Computed densities (g/cm^3) for pure DES and DES/water mixture (80/20% w/w) over last 25 ns of simulation time for each FF used. Average computed diffusion coefficients ($10^{-11} m^2/s$) of the DES components. COM-COM RDF for pure DES model parametrized by FF_{LJ} and $FF_{\pm 0.92e}$. Figures for DCCMs calculated for simulations of HEWL and HEL4 in DES/water mixture (80/20% w/w) parametrized by FF_{LJ} and $FF_{\pm 0.92e}$. Averages of the absolute dynamical cross-correlation value along the diagonal and off diagonal. Minimum distance analysis Trp62-$[Ch]^+$ for HEWL, variation of radius of gyration (R_g) and number of H-bonds of HEL4 as a function of time(PDF)

Acknowledgements

We thank Eric Doorhyee for carrying out PDF measurements. Use of the National Synchrotron Light Source, Brookhaven National Laboratory, was supported by the U.S. Department of Energy, Office of Science, Office of Basic Energy Sciences, under Contract No. DE-AC02-98CH10886 (NSLS-II Proposal Number 306955).

References

[1] A. P. Abbott, G. Capper, G. L. Davies, R. K. Rasheed, and V. Tambyrajah, “Novel solvent

properties of choline chloride/urea mixtures," Chem.Commun., no. 1, pp. 70–71, 2003.

[2] A. Paiva, R. Craveiro, I. Aroso, M. Martins, R. L. Reis, and A. R. C. Duarte, "Natural deep eutectic solvents – solvents for the 21st century," ACS Sustainable Chemistry & Engineering, vol. 2, no. 5, pp. 1063–1071, 2014.

[3] Q. Zhang, K. De Oliveira Vigier, S. Royer, and F. Jerome, "Deep eutectic solvents: syntheses, properties and applications," Chem. Soc. Rev, vol. 41, no. 21, pp. 7108–7146, 2012.

[4] E. L. Smith, A. P. Abbott, and K. S. Ryder, "Deep eutectic solvents (dess) and their applications," Chem. Rev., vol. 114, no. 21, pp. 11 060–11 082, 2014.

[5] C. J. Clarke, W.-C. Tu, O. Levers, A. Bröhl, and J. P. Hallett, "Green and sustainable solvents in chemical processes," Chemical Reviews, vol. 118, no. 2, pp. 747–800, 2018.

[6] B. B. Hansen, S. Spittle, B. Chen, D. Poe, Y. Zhang, J. M. Klein, A. Horton, L. Adhikari, T. Zelovich, B. W. Doherty, B. Gurkan, E. J. Maginn, A. Ragauskas, M. Dadmun, T. A. Zawodzinski, G. A. Baker, M. E. Tuckerman, R. F. Savinell, and J. R. Sangoro, "Deep eutectic solvents: A review of fundamentals and applications," Chemical Reviews, vol. 121, no. 3, pp. 1232–1285, 2021.

[7] M. A. R. Martins, S. P. Pinho, and J. A. P. Coutinho, "Insights into the nature of eutectic and deep eutectic mixtures," J Solution Chem, vol. 48, no. 7, pp. 962–982, 2019.

[8] D. O. Abranches, M. A. R. Martins, L. P. Silva, N. Schaeffer, S. P. Pinho, and J. A. P. Coutinho, "Phenolic hydrogen bond donors in the formation of non-ionic deep eutectic solvents: the quest for type v des," Chem. Commun., vol. 55, no. 69, pp. 10 253–10 256, 2019.

[9] K. Radosevic, M. C. Bubalo, V. G. Srcek, D. Grgas, T. L. Dragicevic, and I. R. Redovnikovic, "Evaluation of toxicity and biodegradability of choline chloride based deep eutectic solvents," Ecotoxicology and Environmental Safety, vol. 112, pp. 46–53, 2015.

[10] Y. P. Mbous, M. Hayyan, A. Hayyan, W. F. Wong, M. A. Hashim, and C. Y. Looi, "Applications of deep eutectic solvents in biotechnology and bioengineering—promises and challenges," Biotechnology Advances, vol. 35, no. 2, pp. 105–134, 2017.

[11] H. Vanda, Y. Dai, E. G. Wilson, R. Verpoorte, and Y. H. Choi, "Green solvents from ionic liquids and deep eutectic solvents to natural deep eutectic solvents," C. R. Chimie, vol. 21, no. 6, pp. 628–638, 2018.

[12] A. P. Abbott, D. Boothby, G. Capper, D. L. Davies, and R. K. Rasheed, "Deep eutectic solvents formed between choline chloride and carboxylic acids: versatile alternatives to ionic liquids," J. Am. Chem. Soc., vol. 126, no. 29, pp. 9142–9147, 2004.

[13] G. García, S. Aparicio, R. Ullah, and M. Atilhan, "Deep eutectic solvents: Physicochemical properties and gas separation applications," Energy & Fuels, vol. 29, no. 4, pp. 2616–2644, 2015.

[14] M. Francisco, A. van den Bruinhorst, and M. C. Kroon, "Low-transition-temperature mixtures (lttms): a new generation of designer solvents," Angew. Chem. Int. Ed., vol. 52, no. 11, pp. 3074–3085, 2013.

[15] C. A. Nkuku and R. J. LeSuer, "Electrochemistry in deep eutectic solvents," J. Phys. Chem. B, vol. 111, no. 46, pp. 13 271–13 277, 2007.

[16] L. Millia, V. Dall'Asta, C. Ferrara, V. Berbenni, E. Quartarone, F. M. Perna, V. Capriati, and P. Mustarelli, "Bio-inspired choline chloride-based deep eutectic solvents as electrolytes for lithium-ion batteries," Solid State Ionics, vol. 323, pp. 44–48, 2018.

[17] J. García-Álvarez, E. Hevia, and V. Capriati, "The future of polar organometallic chemistry written in bio-based solvents and water," Chemistry—A European Journal, vol. 24, no. 56, pp. 14 854–14 863, 2018.

[18] L. Cicco, A. Salomone, P. Vitale, N. Ríos-Lombardía, J. González-Sabín, J. García-Álvarez, F. M. Perna, and V. Capriati, "Addition of highly polarized organometallic compounds to n-tert-butanesulfinyl imines in deep eutectic solvents under air: Preparation of chiral amines of pharmaceutical interest," ChemSusChem, vol. 13, no. 14, pp. 3583–3588, 2020.

[19] F. M. Perna, P. Vitale, and V. Capriati, "Synthetic applications of polar organometallic and alkali-metal reagents under air and moisture," Curr. Opin. Green Sustain. Chem., vol. 30, no. 2452-2236, p. 100 487, 2021.

[20] P. Makoś, E. Słupek, and J. Gębicki, "Hydrophobic deep eutectic solvents in microextraction techniques—A review," Microchemical Journal, vol. 152, p. 104 384, 2020.

[21] R.-T. Zhao, D. Pei, P.-L. Yu, J.-T. Wei, N.-L. Wang, D.-L. Di, and Y.-W. Liu, "Aqueous two-phase systems based on deep eutectic solvents and their application in green separation processes," Journal of Separation Science, vol. 43, no. 1, pp. 348–359, 2020.

[22] F. M. Perna, P. Vitale, and V. Capriati, "Deep eutectic solvents and their applications as green solvents," Curr. Opin. Green Sustain. Chem., vol. 21, no. 2452-2236, pp. 27–33, 2020.

[23] J. T. Gorke, F. Srienc, and R. J. Kazlauskas, "Hydrolase-catalyzed biotransformations in deep eutectic solvents," Chem. Commun., no. 10, pp. 1235–1237, 2008.

[24] P. Xu, G. Zheng, M. Zong, N. Li, and W. Lou, "Recent progress on deep eutectic solvents in biocatalysis," Bioresour. Bioprocess., vol. 4, no. 1, p. 34, 2017.

[25] L. Cicco, G. Dilauro, F. M. Perna, P. Vitale, and V. Capriati, "Advances in deep eutectic solvents and water: Applications in metal- and biocatalyzed processes, in the synthesis of apis, and other biologically active compounds," Org. Biomol. Chem., vol. 19, no. 12, pp. 2558–2577, 2021.

[26] C. Ma, A. Laaksonen, C. Liu, X. Lu, and X. Ji, "The peculiar effect of water on ionic liquids and deep eutectic solvents," Chem. Soc. Rev., vol. 47, no. 23, pp. 8685–8720, 2018.

[27] O. S. Hammond, D. T. Bowron, and K. J. Edler, "The effect of water upon deep eutectic solvent nanostructure: an unusual transition from ionic mixture to aqueous solution," Angew. Chem. Int. Ed., vol. 56, no. 33, pp. 9782–9785, 2017.

[28] T. Zhekenov, N. Toksanbayev, Z. Kazakbayeva, D. Shaha, and F. S. Mjalli, "Formation of type iii deep eutectic solvents and effect of water on their intermolecular interactions," Fluid Phase Equilibria, vol. 441, pp. 43–48, 2017.

[29] P. Kumari, Shobhna, S. Kaur, and H. K. Kashyap, "Influence of hydration on the structure of reline deep eutectic solvent: a molecular dynamics study," ACS Omega, vol. 3, no. 11, pp. 15 246–15 255, 2018.

[30] F. Gabriele, M. Chiarini, R. Germani, M. Tiecco, and N. Spreti, "Effect of water addition on choline chloride/glycol deep eutectic solvents: characterization of their structural and physicochemical properties," J. Mol. Liq., vol. 291, p. 111 301, 2019.

[31] F. Milano, L. Giotta, M. R. Guascito, A. Agostiano, S. Sblendorio, L. Valli, F. M. Perna, L. Cicco, M. Trotta, and V. Capriati, "Functional enzymes in nonaqueous environment: the case of photosynthetic reaction centers in deep eutectic solvents," ACS Sustainable Chem. Eng., vol. 5, no. 9, pp. 7768–7776, 2017.

[32] V. Gotor-Fernández and C. E. Paul, "Deep eutectic solvents for redox biocatalysis," J. Biotechnol., vol. 293, pp. 24–35, 2019.

[33] T. El Achkar, S. Fourmentin, and H. Greige-Gerges, "Deep eutectic solvents: an overview on their interactions with water and biochemical compounds," J. Mol. Liq., vol. 288, p. 111 028, 2019.

[34] B. D. Belviso, F. M. Perna, B. Carrozzini, M. Trotta, V. Capriati, and R. Caliandro, "Introducing protein crystallization in hydrated deep eutectic solvents," ACS Sustainable Chem. Eng., vol. 9, no. 25, pp. 8435–8449, 2021.

[35] M. Bilal, Y. Zhao, S. Noreen, S. Z. H. Shah, R. N. Bharagava, and H. M. N. Iqbal, "Modifying bio-catalytic properties of enzymes for efficient biocatalysis: A review from immobilization strategies viewpoint," Biocatalysis and Biotransformation, vol. 37, no. 3, pp. 159–182, 2019.

[36] A. Sanchez-Fernandez, S. Prevost, and M. Wahlgren, "Deep eutectic solvents for the preservation of concentrated proteins: The case of lysozyme in 1:2 choline chloride:glycerol," Green Chem., vol. 24, no. 11, pp. 4437–4442, 2022.

[37] R. Esquembre, J. M. Sanz, J. G. Wall, F. del Monte, C. R. Mateo, and M. L. Ferrer, "Thermal unfolding and refolding of lysozyme in deep eutectic solvents and their aqueous dilutions," Phys. Chem. Chem. Phys., vol. 15, no. 27, pp. 11 248–11 256, 2013.

[38] A. Sanchez-Fernandez, K. J. Edler, T. Arnold, D. Alba Venero, and A. J. Jackson, "Protein conformation in pure and hydrated deep eutectic solvents," Phys. Chem. Chem. Phys., vol. 19, no. 13, pp. 8667–8670, 2017.

[39] P. Kumari, M. Kumari, and H. K. Kashyap, "How pure and hydrated reline deep eutectic solvents affect the conformation and stability of lysozyme: insights from atomistic molecular dynamics simulations," J. Phys. Chem. B, vol. 124, no. 52, pp. 11 919–11 927, 2020.

[40] A. González de Castilla, J. P. Bittner, S. Müller, S. Jakobtorweihen, and I. Smirnova, "Thermodynamic and transport properties modeling of deep eutectic solvents: a review on ge-models, equations of state, and molecular dynamics," J. Chem. Eng. Data, vol. 65, no. 3, pp. 943–967, 2020.

[41] S. L. Perkins, P. Painter, and C. M. Colina, "Molecular dynamic simulations and vibrational analysis of an ionic liquid analogue," J. Phys. Chem. B, vol. 117, no. 35, pp. 10 250–10 260, 2013.

[42] G. García, M. Atilhan, and S. Aparicio, "The impact of charges in force field parameterization for molecular dynamics simulations of deep eutectic solvents," J. Mol. Liq., vol. 211, pp. 506–514, 2015.

[43] S. L. Perkins, P. Painter, and C. M. Colina, "Experimental and computational studies of choline chloride-based deep eutectic solvents," J. Chem. Eng. Data, vol. 59, no. 11, pp. 3652–3662, 2014.

[44] S. Zahn, B. Kirchner, and D. Mollenhauer, "Charge spreading in deep eutectic solvents," ChemPhysChem, vol. 17, no. 21, pp. 3354–3358, 2016.

[45] S. Mainberger, M. Kindlein, F. Bezold, E. Elts, M. Minceva, and H. Briesen, "Deep eutectic solvent formation: a structural view using molecular dynamics simulations with classical force fields," Mol. Phys., vol. 115, no. 9-12, pp. 1309–1321, 2017.

[46] A. Chaumont, E. Engler, and R. Schurhammer, "Is charge scaling really mandatory when developing fixed-charge atomistic force fields for deep eutectic solvents?" J. Phys. Chem. B, vol. 124, no. 33, pp. 7239–7250, 2020.

[47] E. Lindahl, B. Hess, and D. van der Spoel, "GROMACS 3.0: a package for molecular simulation and trajectory analysis," J. Mol. Model., vol. 7, no. 8, pp. 306–317, 2001.

[48] D. van der Spoel, E. Lindahl, B. Hess, G. Groenhof, A. Mark, and H. Berendsen, "GROMACS: fast, flexible, and free.," J. Comput. Chem., vol. 26, no. 16, pp. 1701–1718, 2005.

[49] L. Martínez, R. Andrade, E. G. Birgin, and J. M. Martínez, "Packmol: A package for building initial configurations for molecular dynamics simulations," J. Comput. Chem., vol. 30, no. 13, pp. 2157–2164, 2009.

[50] P. J. Artymiuk, C. C. F. Blake, D. W. Rice, and K. S. Wilson, "The structures of the monoclinic and orthorhombic forms of hen egg-white lysozyme at 6 Å resolution," Acta Crystallogr. B, vol. 38, no. 3, pp. 778–783, 1982.

[51] J. Wang, R. M. Wolf, J. W. Caldwell, P. A. Kollman, and D. A. Case, "Development and testing of a general amber force field," J. Comput. Chem., vol. 25, no. 9, pp. 1157–1174, 2004.

[52] Y. Duan, C. Wu, S. Chowdhury, M. C. Lee, G. Xiong, W. Zhang, R. Yang, P. Cieplak, R. Luo, T. Lee, J. Caldwell, J. Wang, and P. Kollman, "A point-charge force field for molecular mechanics simulations of proteins based on condensed-phase quantum mechanical calculations," J. Comput. Chem., vol. 24, no. 16, pp. 1999–2012, 2003.

[53] M. J. Frisch, G. W. Trucks, H. B. Schlegel, G. E. Scuseria, and *et al.*, "Gaussian 16," Revision B.01 (Wallingford, CT: Gaussian, Inc.), 2016.

[54] R. B. Leron, A. N. Soriano, and M. H. Li, "Densities and refractive indices of the deep eutectic solvents (choline chloride+ethylene glycol or glycerol) and their aqueous mixtures at the temperature ranging from 298.15 to 333.15k," J. Taiwan Inst. Chem. Eng., vol. 43, no. 4, pp. 551–557, 2012.

[55] R. B. Leron, D. S. H. Wong, and M. H. Li, "Densities of a deep eutectic solvent based on choline chloride and glycerol and its aqueous mixtures at elevated pressures," Fluid Phase Equilibria, vol. 335, pp. 32–38, 2012.

[56] I. S. Joung and T. E. Cheatham, "Determination of alkali and halide monovalent ion parameters for use in explicitly solvated biomolecular simulations," J. Phys. Chem. B, vol. 112, no. 30, pp. 9020–9041, 2008.

[57] W. L. Jorgensen, J. Chandrasekhar, J. D. Madura, R. W. Impey, and M. L. Klein, "Comparison of simple potential functions for simulating liquid water," J. Chem. Phys., vol. 79, no. 2, pp. 926–935, 1983.

[58] T. Darden, D. York, and L. Pedersen, "Particle mesh ewald: an n·log(n) method for ewald sums in large systems," J. Chem. Phys., vol. 98, no. 12, pp. 10 089–10 092, 1993.

[59] B. Hess, H. Bekker, H. J. C. Berendsen, and J. G. E. M. Fraaije, "LINCS: a linear constraint solver for molecular simulations," J. Comput. Chem., vol. 18, no. 12, pp. 1463–1472, 1997.

[60] G. Bussi, D. Donadio, and M. Parrinello, "Canonical sampling through velocity rescaling," J. Chem. Phys., vol. 126, no. 1, p. 014 101, 2007.

[61] M. Parrinello and A. Rahman, "Polymorphic transitions in single crystals: A new molecular dynamics method," J. Appl. Phys., vol. 52, no. 12, pp. 7182–7190, 1981.

[62] S. Nosé and M. L. Klein, "Constant pressure molecular dynamics for molecular systems," Mol. Phys., vol. 50, no. 5, pp. 1055–1076, 1983.

[63] S. Nosé, "A molecular dynamics method for simulations in the canonical ensemble," Molecular Physics, vol. 52, no. 2, pp. 255–268, 1984.

[64] W. G. Hoover, "Canonical dynamics: equilibrium phase-space distributions," Phys. Rev. A, vol. 31, no. 3, pp. 1695–1697, 1985.

[65] A. P. Hammersley, S. O. Svensson, M. Hanfland, A. N. Fitch, and D. Hausermann, "Two-dimensional detector software: From real detector to idealised image or two-theta scan," High Pressure Research, vol. 14, no. 4-6, pp. 235–248, 1996.

[66] P. Juhás, T. Davis, C. Farrow, and S. Billinge, "Pdfgetx3: A rapid and highly automatable program for processing powder diffraction data into total scattering pair distribution functions," J. Appl. Crystallogr., vol. 46, no. 2, pp. 560–566, 2013.

[67] P. Juhás, C. L. Farrow, X. Yang, K. R. Knox, and S. J. L. Billinge, "Complex modeling: A strategy and software program for combining multiple information sources to solve ill posed structure and nanostructure inverse problems," Acta Crystallogr., Sect. A, vol. 71, no. 6, pp. 562–568, 2015.

[68] M. Allen and D. Tildesley, Computer Simulation of Liquids. Oxford University Press, 1987.

[69] W. Humphrey, A. Dalke, and K. Schulten, "Vmd: visual molecular dynamics," J. Mol. Graph., vol. 14, no. 1, pp. 33–38, 1996.

[70] R. Brun and F. Rademakers, "Root: An object oriented data analysis framework," Nucl. Inst. & Meth. in Phys. Res. A, vol. 389, pp. 81–86, 1997.

[71] C. D'Agostino, R. C. Harris, A. P. Abbott, L. F. Gladden, and M. D. Mantle, "Molecular motion and ion diffusion in choline chloride based deep eutectic solvents studied by 1h pulsed field gradient nmr spectroscopy," Phys. Chem. Chem. Phys., vol. 13, no. 48, pp. 21 383–21 391, 2011.

[72] A. Yadav, S. Trivedi, R. Rai, and S. Pandey, "Densities and dynamic viscosities of (choline chloride+glycerol) deep eutectic solvent and its aqueous mixtures in the temperature range (283.15–363.15)k," Fluid Phase Equilibria, vol. 367, pp. 135–142, 2014.

[73] A. H. Turner and J. D. Holbrey, "Investigation of glycerol hydrogen-bonding networks in choline chloride/glycerol eutectic-forming liquids using neutron diffraction," Phys. Chem. Chem. Phys., vol. 21, no. 39, pp. 21 782–21 789, 2019.

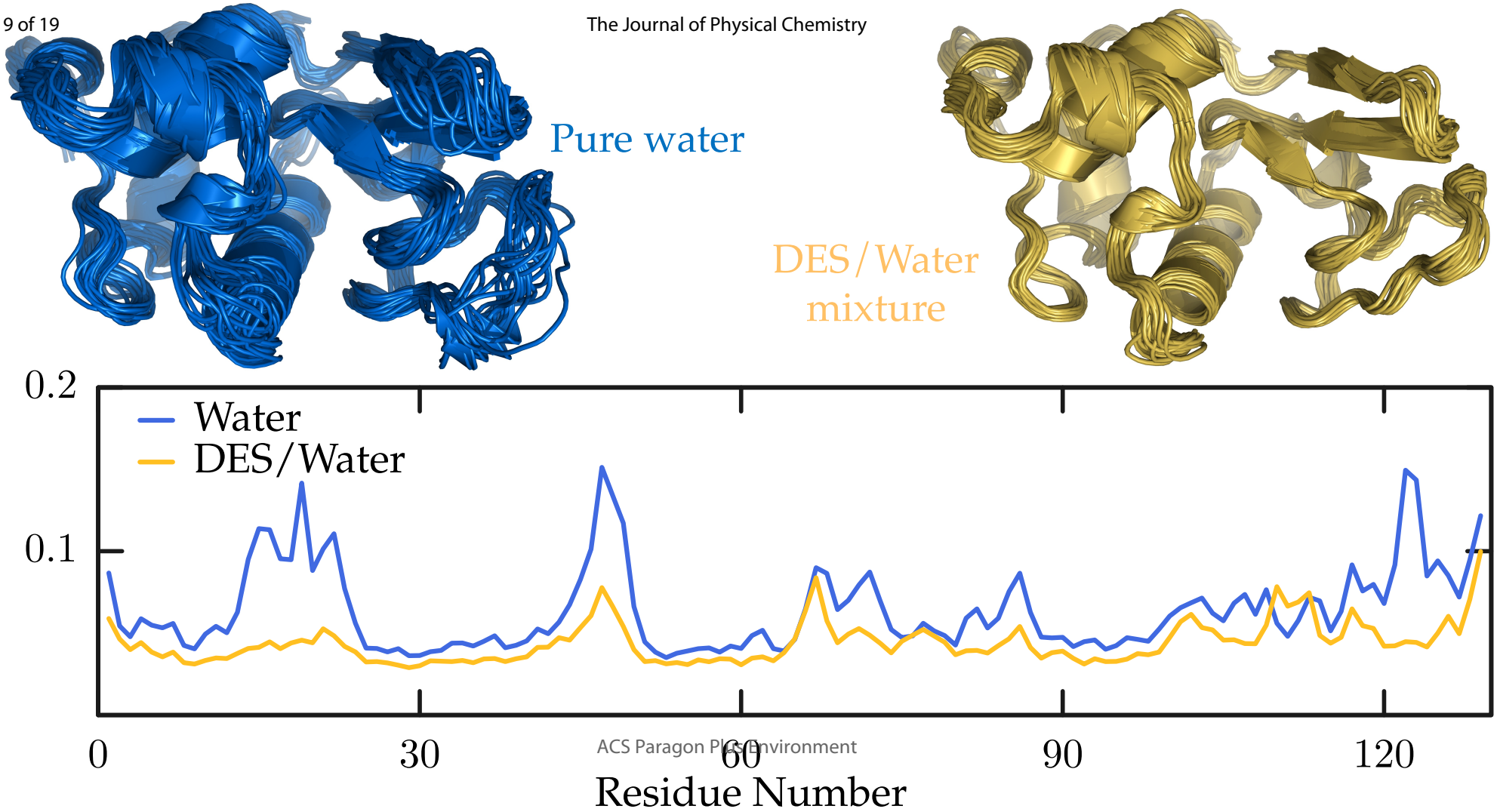
Pure water
DES/Water mixture
Water
DES/Water
RMSF (nm)
0.2
0.1
0
30
60
90
120
Residue Number